

THE SLOW KINETICS OF ELEMENTARY CALCIUM EVENTS IN *XENOPUS* OOCYTES

IRINA BĂRAN

Biophysics Department, "Carol Davila" University of Medicine and Pharmaceutics, 8, Eroilor
Sanitari Blvd, 050474 Bucharest, Romania

Abstract. A possible way to explain the difference between theory and experiment with regard to the slow kinetics of elementary calcium events visualized by lateral scanning in *Xenopus* oocytes is to assume that the Ca^{2+} source is located on the surface of tubules of the endoplasmic reticulum and the image is not captured frontally, but on the opposite side of a tubule. Our results obtained with this release-detection configuration concur with a distribution of functional inositol 1,4,5-trisphosphate receptors disposed as clusters at depths of either 2.5 or 6.5 μm under the plasma membrane. This arrangement can explain why fast transients are detected on radial but not lateral direction and reproduces accurately the time scale, spatial size, fluorescence amplitude and other features of Ca^{2+} transients. The model suggests that the radial distribution of operative receptors should be estimated by selecting fast calcium events detected by axial scanning. Geometry that breaks spherical symmetry determines large differences in the estimation of release fluxes. Isotropic diffusion-based methods may overestimate with one order of magnitude both the duration and the amount of released Ca^{2+} but the current amplitude may be correct. Contrary to previous interpretation, fluorescence intensity does not begin to decay until the calcium current turns off.

Key words: calcium release, inositol 1,4,5 trisphosphate, *Xenopus* oocyte, line scanning, anisotropic diffusion, model.

INTRODUCTION

An intriguing issue on Ca^{2+} release is the kinetics of the biphasic Ca^{2+} signals recorded locally as individual, 'elementary' events arising at discrete sites inside the cell [3, 4, 8]. The calcium release units represent compact clusters of inositol 1,4,5-trisphosphate receptors (IP_3Rs), which function as Ca^{2+} channels of the endoplasmic reticulum (ER). In *Xenopus* oocytes both the rise and decay phases of these Ca^{2+} transients, detected by line scan imaging, appear to be about ten-fold slower (half-decay: $t_{1/2} \sim 0.1$ s) than expected from analytical calculations and numerical simulations [6, 7, 9] where either the channel's mouth is considered as a point source placed in the center of the space or multiple sources are distributed on a planar ER region. In different configurations that assume cylindrical geometry around tubules or disc pieces of the ER, the decay presents two dominant

Received: December 2005;
in final form January 2006.

exponential components of about 1–3 ms and 12–40 ms if the calcium transient is investigated at its release site [10] or averaged radially over a 2 μm distance from the release site [1]. The kinetics appears slower, with decay time constant of 200 ms, at larger distances, of 2.5 μm , from the Ca^{2+} source [10], but in these particular geometries the relation to the spatial size of the event has not been investigated. This is an important point because it has been argued that sharp images cannot be obtained far from the release site [8].

Interestingly, the decay phase of the release events ('sparks') detected in heart cells is faster, with half-decay time ~ 20 ms [7]. Numerical simulations [5, 7] that consider a virtual point Ca^{2+} source and cytosolic buffering and diffusion conditions similar to the *Xenopus* case [9] return values close to the experimental ones. Even in a cylindrical geometry that assumes release from a source distributed over a ring of 0.3 μm radius, simulations that include optical blurring of the image do not differ significantly from those with spherical symmetry [7]. Upon lowering with one order of magnitude the rate of Ca^{2+} binding to the indicator, $t_{1/2}$ can increase to 49 ms [7]. Longer decay times may be also obtained by increasing the distance from the source to the scan line, but this is equivalent to remaining in the low-amplitude domain of the fluorescent signal [5, 7], which is not the case with *Xenopus*. Here, the fluorescence amplitude relative to the resting fluorescence reaches values as high as 3.5, with most frequent values between 1.5 and 2.4 [8]. The half-decay time ($t_{1/2}$) of fluorescence signals associated to local calcium transients in *Xenopus* oocytes was systematically found in the range 60–140 ms with focusing at submembrane depths of 3–6 μm where the IP_3Rs are located [3, 4, 8]. A presumptive wide organelle that would act ubiquitously as a barrier for diffusion [9] appears unrealistic to the oocyte morphology [3]. In repeated recordings, contrary to the situation indicated by results of Izu *et al.* [5], low $t_{1/2}$ values appear to correspond to low amplitudes obtained with short events (conventionally termed 'blips') [8], while high amplitude events ('puffs') decay more slowly. This situation has been obtained to a lesser extent in [7] by varying the release duration or the source strength, but $t_{1/2}$ remains below 40 ms. Noise has been found to affect the decay constant of local fluorescence signals [5]. With the system used for investigating sparks in ventricular cells, Izu *et al.* [5] found a Gaussian distribution of noise values, whereas with the system used in recordings on *Xenopus* oocytes [8] the fluctuations appear to be rather independent of the signal amplitude. Our simulations using noise defined in this way exclude signal fluctuations as a possible cause of the apparently high $t_{1/2}$ in *Xenopus* oocytes.

To date, all of the existent calculations have been made on the assumption that the image of the calcium event is taken at variable distances in front of the source. We use an alternative geometry of Ca^{2+} release. We have shown [1] it can explain the intralumenal $\text{Ca}^{2+}/\text{K}^+$ exchange as well as in- or out-of-phase oscillations observed locally in the lumen and the cytosol of permeabilized cells. A generic release event is considered as a simultaneous opening of channels located on ER tubules of 300–400 nm radius, and the event image is reconstructed with blurring included.

METHODS

To simulate release at individual sites we apply the procedure presented in full detail in [1], and use Scenario II therein. For simplicity, the K^+ gradient across the ER membrane is set to zero. We consider a cluster of IP_3Rs placed on a tubule of the ER with radius of 300–400 nm and calculate the time and space variation in the various species concentration following the simultaneous opening of 1–25 channels. Clustered IP_3Rs are configured in a regular lattice with 75 nm mesh on the surface of the ER tubule cylinder. The tubule segment length considered in simulations is 9 μm . Using either periodic or fixed boundary conditions at the z edges does not produce significant differences in the kinetics of the release event. At the radial edge of the simulated cytosolic volume depth (4 μm from the tubule membrane) fixed boundary conditions (with $[\text{Ca}^{2+}] = 140 \text{ nM}$) are applied. The Laplacean is discretized in cylindrical coordinates, with spatial steps $\Delta y = \Delta r = 75 \text{ nm}$.

The reaction-diffusion equations are solved with an explicit finite difference formula in cylindrical coordinates. Both endo- and exogenous (Calcium Green-1) mobile buffers are included in the simulations, with respective total concentration of 50 μM and 40 μM , dissociation constant 10 μM and 0.7 μM , on-rate constant 10 $\mu\text{M}^{-1}\text{s}^{-1}$ and 500 $\mu\text{M}^{-1}\text{s}^{-1}$, and diffusion coefficient 15 $\mu\text{m}^2/\text{s}$ and 18.4 $\mu\text{m}^2/\text{s}$, respectively. The endogenous fix buffer is present with a total concentration 300 μM , $K_d = 10 \mu\text{M}$ and $k^{\text{on}} = 50 \mu\text{M}^{-1}\text{s}^{-1}$. Ca^{2+} is assumed to have a diffusion coefficient of 220 $\mu\text{m}^2/\text{s}$. All concentrations and the total current intensity are averaged every 1 ms. The basal value of cytosolic $[\text{Ca}^{2+}]$ of 140 nM is calculated by equating $\Delta F/F_0 = 5$ in the presence of saturating Ca^{2+} [8].

In order to describe elementary calcium events detected by linescan imaging, the scan line is assumed to span the cytosol on a direction either parallel or transverse to the ER tubule, at a distance of 150–250 nm from the tubule membrane. For simplicity the ER tube is assumed to be parallel to the plasma membrane. Lateral and axial linescanning refers to the situations where the scan line is either parallel or perpendicular to the plasma membrane, respectively [3, 8]. Axial events are therefore recorded along a radial direction that crosses the cell nucleus, whereas lateral events evolve in a plane that is parallel to the cell membrane. The center of the cluster of IP_3 receptor channels is oriented under a variable angle α with respect to the center of the scan line. Both centers are in the plane $y = 0$. The center, O, of the tubule segment, is considered the origin of the coordinate system. The formation of the blurred optical image is simulated following published procedures [5, 7] converted to cylindrical coordinates. The point spread function of the confocal microscope is defined with a three-dimensional Gaussian function with lateral and axial confocal full-width at half-maximum (FWHM) set here to 250 nm and 400 nm, respectively [8]. At every instant, the resulting linear image is obtained by calculating, at discrete locations along the scan line, the fluorescence contribution of all of the spatial elements modulated by the value of the point spread function associated to each element [5,

7]. The fluorescence originating from the interior of the tubule is assumed to be constant and equal to the resting fluorescence, because no significant inhomogeneities have been detected in *Xenopus* oocytes [3, 8]. In the case of transverse orientation of the scan line, the discrete locations are determined by the intersection of the scan line with any spatial element that has its center at an axial distance ≤ 50 nm from the scan line. The scan line is divided in 100 nm-length segments. Their centers define the position, d , along the scan line. At a given position d , there may be several spatial elements that intersect the parallelepiped associated to the scan line, and the quantity associated to the fluorescence signal is spatially averaged over these elements. All such elements have $dy = 75$ nm, which is exactly the Δy -step of the spatial discretization. The center of the release event is fixed at the highest local increase in the fluorescence value detected on the scan line, and the fluorescence profile is calculated and averaged around that center over a distance of 400 nm along the scan line [4, 8].

Actual and expected mass traces related to the fluorescence signal are estimated by integrating $\Delta F/F_0$ over the whole cytosolic volume considered in simulations, and, respectively, by the method of Sun *et al.* [8], i.e. by summing the fluorescence signals ($\Delta F/F_0$) along the scan line, weighted by the third power of the distance from the respective volume element to the center of the event. Total and local quantities associated with fluorescence signals ΔF are referred to values corresponding to the cytosolic domain of the simulation, and to quantities averaged around the center of the event, respectively. Actual $\Delta[\text{Ca}^{2+}]$ (total) is obtained by integrating $\Delta[\text{Ca}^{2+}]$ over the simulated cytosolic volume.

Various fluorescence amplitudes in the right domain [3, 4, 8] were obtained with detection angles of 110° – 160° by varying the number of open channels (between 1 and 25), the release duration (3–300 ms), and the tubule radius (300–400 nm) in a large number of simulations. The current intensity varies during release, but reaches a quasisteady state in a few milliseconds. It is determined by the intrinsic local dynamics of calcium ions on the two sides of the reticulum membrane at the location of the cluster. The dynamic equations are described in detail in [1]. The availability of free calcium at the luminal side of the receptor is a determinant factor of the source strength, and, implicitly, of the fluorescence signal. Extremely bright images ($F/F_0 > 3$) could be obtained with total ionic currents ≥ 4 pA, which require here a luminal stationary Ca^{2+} content of 2.0–2.5 mM.

RESULTS

THE CORRECT DYNAMICS IS OBTAINED WITH $\alpha = 110^\circ$ – 160°

The detection angle dependence of the fluorescence signal is typically obtained as in Fig. 1. The decay of the simulated fluorescence signal after channel closure is the most rapid (half-decay time 10–25 ms) when the linescan image is

captured in the front of the cluster ($\alpha = 0^\circ$, or frontal detection), and the slowest (half-decay time 60–140 ms) on the opposite side of the tubule ($\alpha \sim 180^\circ$). In numerous simulations we performed, the kinetics of the simulated signals matched the desired profile only with 110° – 160° viewing and tube radius between 300 and 375 nm. The calcium events simulated here present apparent radial diffusion as if calcium would be liberated from a point source in a spherically symmetric space, in the same way the experimental findings indicate [8].

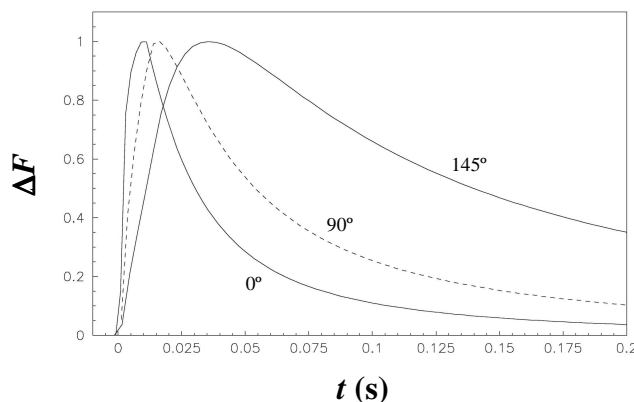


Fig. 1. Fluorescence signals, normalized to the maximum, obtained with different orientations of the lateral scan line (0° , 90° or 145° detection angle), for a 300 nm-radius ER tubule. The maximum total ionic current is 3.44 pA, the release lasts for 20 ms, and the number of open channels is nine. The maximum signal intensity (F_{\max}/F_0) detected at 145° orientation of the scan line is 2.5.

REAL VERSUS EXPECTED KINETICS OF Ca^{2+} RELEASE

Ca^{2+} kinetics is not accessed directly in experiments, but through determination of time variation in the fluorescence of a calcium binding dye. The currently accepted interpretation of the *Xenopus* data is that calcium liberation persists even during the falling phase of the fluorescence signal and that the slow fluorescence rise (time at half amplitude ~ 50 ms) reflects a progressive increase in calcium channel conductance [8]. Afterwards the resolving of the radial receptor distribution raised certain questions on the calculation method, but it was still assumed that the errors introduced by deeper release sites should be small [3]. We investigated these possibilities and analyzed the relation between the signal mass [8] and the observed fluorescence signal. At present, signal mass is considered the most reliable quantity that can be derived from a local fluorescence signal. Signal mass is calculated on the basis of the spherical symmetry assumption and is currently considered to give a measure of the Ca^{2+} flux that generates the local calcium transient. We calculated the signal mass by the procedure of Sun *et al.* [8] and obtained a similar slowing down of the signal mass profile compared to the fluorescence trace, as it was observed in experiments. This slowing down

determines the prolongation of the signal mass increase even after channels' closure. If our hypothesis applies, the prolonged rise phase of the estimated mass profile can be caused by anisotropic diffusion in the particular geometry of release and signal detection, and fluorescence would not begin to decay until the calcium current turns off. Therefore, the estimated signal mass might be not a true measure of the amount of calcium liberated as proposed [8], and Fig. 2 shows the difference between the actual and the expected increase in the free calcium amount, for a 145° orientation of the scan line.

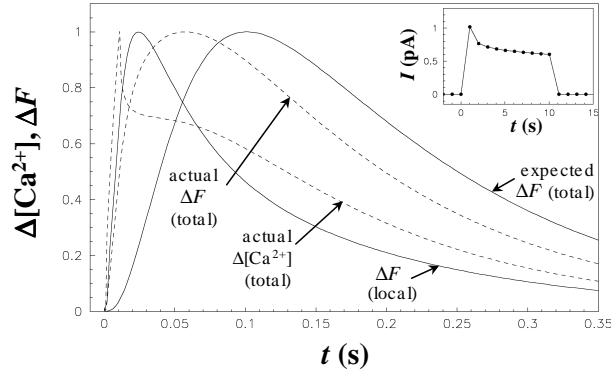


Fig. 2. Actual *versus* expected kinetics of local calcium ($[Ca^{2+}]$) and fluorescence (ΔF) signals normalized to their maximal values (here F_{max}/F_0 is 1.48). Inset shows the total Ca^{2+} current through the cluster of nine IP_3Rs during the conduction period of 10 ms.

SPATIAL ORGANIZATION OF IP_3Rs

Previous investigations revealed a condensation of IP_3Rs on two bands centered around 3 and 6 μm under the cell membrane of the *Xenopus* oocyte [3]. Because the minimum half-decay time of Ca^{2+} events recorded at 3–6 μm depth is $\cong 60$ ms [3, 4, 8], we speculate, based on our determinations, that no release event is detected frontally inside this region. According to our model, the IP_3 receptors at this location should be inoperative, whereas the functional receptors should be disposed as clusters at two distinct depths into the cell, of about 2.5 and 6.5 μm , respectively. Clusters outputs should be predominantly oriented either toward the plasma membrane if they are located on the external shell or toward the cell nucleus, otherwise.

According to this scenario, axial scanning should detect both fast and slow events, which already have been found [3] (see e.g., Fig. 3D in [3]). The experimental radial distribution of calcium events does not disagree with our hypothesis, although most puffs have been detected axially at depths between about 4 and 6 μm [3], where we propose that no release event arises. We found by simulation that such puffs can be obtained as projections on a radial direction in the

back of the ER tubule and, in consequence, present slow kinetics. A selection of fast axial events (i.e., with $t_{1/2} < 40$ ms) should approximate the real distribution of functional receptors, since these events only are viewed close to the release site.

We simulated axial calcium events with the same procedure but with axial FWHM of $0.7 \mu\text{m}$ [3]. In this case the orientation of the scan lines is considered as in Fig. 3. The position and kinetics of detected images of the release events depend largely on the line scan orientation. Axial images captured frontally to the cluster are faster, while those captured from the back are slower. A large number of puffs with appearance of double-site release events [3] can be explained by an arrangement of IP_3 receptors predominantly close to the median plane of the tubule, like in Fig. 3. We were able to reproduce them under the same conditions as those defining the left scan line shown in Fig. 3 (not shown).

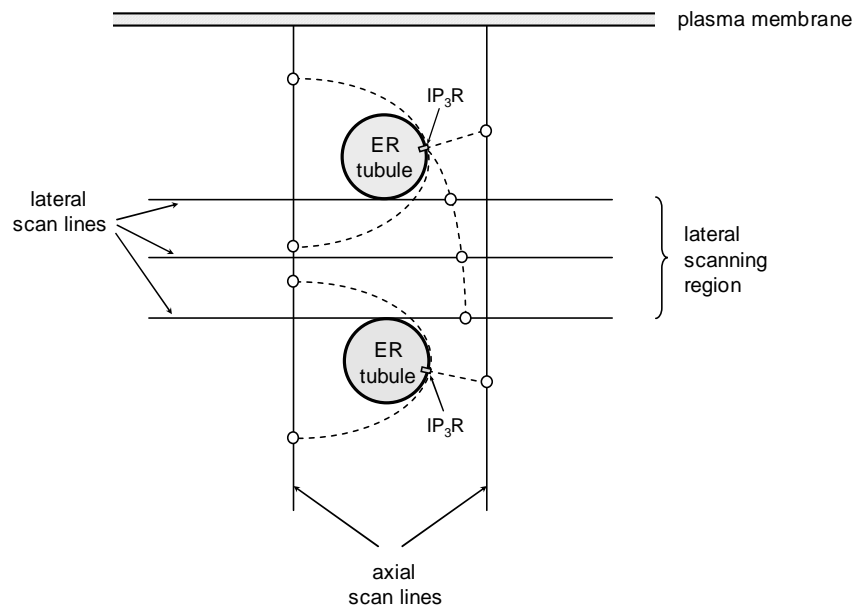


Fig. 3. Release-detection configuration. Dashed lines represent Ca^{2+} ions trajectories that determine highest local ΔF (i.e., the center of the puff, marked by open circles) on a certain scan line. These traces and all spatial quantities are qualitative only. ER tubules are parallel to the plasma membrane; gray circles are transverse sections of the tubules. For clarity in representing axial events, radial scan lines are common to both tubules, which are aligned at the same lateral coordinates. A single Ca^{2+} channel (IP_3R) is represented at the surface of each tubule.

In addition, the fact that the highest frequency of single events [3] was observed in the region denoted in Fig. 3 ‘lateral scanning region’ suggests also a predominant distribution of channels close to the median plane of the tubule ($\alpha \cong 110^\circ$, constrained by results on lateral events). The numerous observations of double release events by axial scanning [3] add more evidence in favor of our

hypothesis. Apparently double events are predicted by our model as single-site events detected with 160° – 200° axial viewing, i.e. $\alpha = 70^\circ$ – 110° (results not shown). The radial spacing between presumptive coupled release sites has been estimated to be $1.63\ \mu\text{m}$ because the width distribution of single and apparently double events peaks at $1.62\ \mu\text{m}$ and $3.25\ \mu\text{m}$, respectively [3]. We also obtained (on average) this value for the distance between centers of coupled puffs on a radial scan line (e.g., left line in Fig. 3). Our results suggest that the frequency of real double events was overestimated (calculated from data it resulted 2.5 relative to the single-event frequency [3]). Random positioning of the axial scan line relative to the ER tubes implies an almost 0.5 probability that a single-site event has the appearance of a double event (it depends on line orientation and distance to the tube, Fig. 3). With this approximation, single- and apparent double-events have the same frequency, so real double events would be then 0.75, not 2.5, as frequent as single events. In case that two ER tubes are close enough, three coupled site events are expected to appear onto the image. For example, assuming the situation on the left side of Fig. 3, the two centers in the middle will be indistinguishable, so the image will appear with three distinct sites. There is some evidence for triple events but unfortunately the data are not sufficient for characterization of multiple release-like events [3].

CONCLUSION

In this paper we propose the hypothesis that elemental calcium events observed in *Xenopus* oocytes by lateral scanning of a restricted region close to the plasma membrane are images obtained with fluorescence signals received from distant release sites, situated on the back of ER tubes. By numeric simulations that include optical blurring of the image, we show that this release-detection geometry can reproduce salient features of calcium events, such as slowness of signal decay, rising phase, spatial size, apparent diffusion like from a point source in a spherically symmetric space, fluorescence amplitude and time to reach steady state.

We compare the observed release kinetics with that predicted as real. Simulations show that fluorescence measurements may not reproduce the actual dynamics of free Ca^{2+} , mainly because the dye is not at equilibrium with Ca^{2+} and fluorescence is delayed by the time it takes for Ca^{2+} , dye and buffers to diffuse to the scan line, but also because there is no available method to evaluate the real signal mass profile from imaging data, other than the spherical approximation. If our hypothesis comes out to be true, this approximation leads, within the *Xenopus* oocyte system, to large overestimation of both release duration and the quantity of released calcium, although the Ca^{2+} current amplitude may be correct.

Reproduction of observed kinetics is acquired with calcium in concentration of 2.0–2.5 mM in the lumen and single channel currents between 0.07 and 0.4 pA. In connection with this, the physiological unitary IP_3R current established with 2.5 mM luminal calcium has been predicted earlier to be about 0.5 pA [9]. On the other hand, our results are compatible with other recent predictions of about 0.08–

0.3 pA at 2.5 mM luminal calcium [10]. Given a release flux of about 4 pA, we estimate that at least 10 IP_3Rs must be activated during an extremely bright puff, while for medium amplitude puffs, of 2.5 pA [8], at least 6 channels must release Ca^{2+} . This figure is similar to that estimated by Sun *et al.* [8], who, based on the unitary flux of about 0.5 pA, deduced that 5–8 channels should conduct Ca^{2+} during large puffs. However, the number of six open channels is obtained with the largest capture radius of the pore (12 nm), which is not a purely geometric quantity, but additionally depends on factors involving ion diffusion at the channel mouth and on the size of the volume within which negative charges surrounding the central pore are located. We previously found that values between 4 and 12 nm are required to explain local oscillations in permeabilized cells [1]. It is most likely however that the radius is smaller (≤ 9 nm) in the actual configuration of the IP_3 receptor, so the number of conducting IP_3Rs should be accordingly higher. Other recent model simulations [10] used a smaller radius of 6 nm. On average, on account of a 8 nm radius, we could best reproduce medium and very bright puffs with 9–12 and 16–25 open channels, respectively, and with single channel currents < 0.28 pA. Since at present there is no available technique to allow direct determination of cluster activity during release, theoretical models use indirect evaluation of release currents and number of conducting channels in a cluster. Our results argue that, in order to gain new insights into the release process *in vivo*, distortion of these quantities by geometry without spherical symmetry should be reconsidered.

Our model requires quite large (300 nm radius) tubular structures of the ER to predominate in the vicinity of the plasma membrane of the oocyte, compared with the more reduced size (up to 30 nm radius) of network ER tubes in a liver cell, but closer to the recently found ~ 300 nm diameter in cardiac cells. Further investigations are needed to clarify the structure of superficial ER in the large-sized oocyte of *Xenopus*.

Two model predictions have been confirmed so far. One, axial scanning reveals both fast and slow events, implying that the observed kinetics depends on the line scan position relative to the release site. Two, the model predicts that, by random orientation of the scan line, double-site events should be detected. Actually they have been observed with high frequency in axial scan images [3]. We suggest a model for the spatial organization of the functional IP_3Rs (Fig. 3) that could explain major findings in *Xenopus* oocytes. The distribution of IP_3Rs capable of releasing Ca^{2+} should be obtained by selecting only fast events from the data obtained with axial scanning.

The results presented here suggest that Ca^{2+} flux reconstruction from fluorescence imaging data can be substantially distorted by the presence of diffusion barriers introduced by the ER itself. According to our model, anisotropic diffusion can account for the observed spatial size (3–4 μm) [3, 4, 8] of elemental events in both lateral and axial recordings, which is almost two times larger than estimated with isotropic diffusion. In muscle cells the size discrepancy has been explained by spatial expansion of the source, but in *Xenopus* oocytes this

representation cannot clarify the origin of the slow time scale for many bright release events.

In conclusion, we provide a possible explanation for the appearance of both fast and slow puffs observed in *Xenopus* oocytes, as well as for their large size. The hypothesis we propose is testable in some respects, but most important, lends support for further experimental and theoretical investigations intended to elucidate the mechanisms of release. Improved fluorescent indicators, better resolution in image acquisition and incorporation of barriers for diffusion in reconstruction algorithms will certainly extend our knowledge of how Ca^{2+} is released from the ER *in vivo*. For a complete understanding, the IP_3R behavior *in vivo* must also be found out. To date no experimental or theoretical results indicate how the IP_3R is actually functioning in intact cells. In another work [2] we propose a model that predicts the IP_3R activity *in vivo*. Future access to the exact description of the calcium release dynamics will provide a new basis for the study of various physiological processes that depend on Ca^{2+} .

REFERENCES

1. BĂRAN, IRINA, Integrated luminal and cytosolic aspects of the calcium release control, *Biophys. J.*, 2003, **84**, 1470–1485.
2. BĂRAN, IRINA, Gating mechanisms of the type 1 inositol 1,4,5-trisphosphate receptor, *Biophys. J.*, 2005, **89**, 979–998.
3. CALLAMARAS, N., I. PARKER, Radial localization of inositol 1,4,5-trisphosphate-sensitive Ca^{2+} release sites in *Xenopus* oocytes resolved by axial confocal linescan imaging, *J. Gen. Physiol.*, 1999, **113**, 199–213.
4. CALLAMARAS, N., I. PARKER, Phasic characteristic of elementary Ca^{2+} release sites underlies quantal responses to IP_3 , *EMBO J.*, 2000, **19**, 3608–3617.
5. IZU, L.T., W.G. WIER, C.W. BALKE, Theoretical analysis of the Ca^{2+} spark amplitude distribution, *Biophys. J.*, 1998, **75**, 1144–1162.
6. NARAGHI, M., E. NEHER, Linearized buffered Ca^{2+} diffusion in microdomains and its implication for calculation of $[\text{Ca}^{2+}]$ at the mouth of a calcium channel, *J. Neurosci.*, 1997, **17**, 6961–6973.
7. SMITH, G.D., J.E. KEIZER, M.D. STERN, W.J. LEDERER, H. CHENG, A simple numerical model of calcium spark formation and detection in cardiac myocytes, *Biophys. J.*, 1998, **75**, 15–32.
8. SUN, X.-P., N. CALLAMARAS, J.S. MARCHANT, I. PARKER, A continuum of InsP_3 mediated elementary Ca^{2+} signalling events in *Xenopus* oocytes, *J. Physiol.*, 1998, **509**, 67–80.
9. SWILLENS, S., P. CHAMPEIL, L. COMBETTES, GENEVIEVE DUPONT, Stochastic simulation of a single inositol 1,4,5-trisphosphate-sensitive Ca^{2+} channel reveals repetitive openings during 'blip-like' Ca^{2+} transients, *Cell Calcium*, 1998, **23**, 291–302.
10. THUL, R., M. FALCKE, Release currents of IP_3 receptor channel clusters and concentration profiles, *Biophys. J.*, 2004, **86**, 2660–2673.